Fatigue strength of additively manufactured polylactide (PLA): effect of raster angle and non-zero mean stresses

O. H. Ezeh and L. Susmel

Department of Civil and Structural Engineering, The University of Sheffield, Mappin Street, Sheffield, S1 3JD, United Kingdom

Corresponding Author: Prof. Luca Susmel
Department of Civil and Structural Engineering
The University of Sheffield, Mappin Street, Sheffield, S1 3JD, UK
Telephone: +44 (0) 114 222 5073
Fax: +44 (0) 114 222 5700
E-mail: l.susmel@sheffield.ac.uk

ABSTRACT

As far as polymers are concerned, polylactide (PLA) is certainly the polymeric compound that is most commonly used along with commercial additive manufacturing technologies. In this context, the present paper aims to investigate the influence of manufacturing direction and superimposed static stresses on the fatigue strength of PLA 3D-printed by using the Fused Filament Fabrication technique. This was done not only by generating a large number of new experimental results, but also by re-analysing different data sets taken from the technical literature. As long as the fused deposition modelling technology is used to fabricate, flat on the build-plate, objects of PLA, the obtained results and the performed re-analyses allowed us to come to the following conclusions: (i) the influence of the manufacturing direction can be neglected with little loss of accuracy; (ii) the effect of superimposed static stresses can be quantified and assessed effectively by simply performing the fatigue assessment in terms of maximum stress in the cycle; (iii) if appropriate experiments cannot be run, AM PLA can be designed against fatigue (for a probability of survival larger than 90%) by referring to a unifying design curve having negative inverse slope equal to 5.5 and endurance limit (at $=2 \cdot 10^6$ cycles to failure) equal to 10% of the material ultimate tensile strength.

Keywords: additive manufacturing, polylactide (PLA), mean stress effect, fatigue design

Nomenclature

k   negative inverse slope

E   Young's modulus

N_{Ref} reference number of cycles to failure

P_S probability of survival

R   load ratio ($R=\sigma_{min}/\sigma_{max}$)

S_D standard deviation

T_σ scatter ratio of the endurance limit for 90% and 10% probabilities of survival

θ_p manufacturing angle

σ_{UTS} ultimate tensile strength

σ_a stress amplitude

σ_A amplitude of the endurance limit extrapolated at N_{Ref} cycles to failure

σ_m mean stress

σ_M mean value of the endurance limit extrapolated at N_{Ref} cycles to failure

σ_{max} maximum stress in the cycle

σ_{MAX} maximum value of the endurance limit extrapolated at N_{Ref} cycles to failure

σ_{min} minimum stress in the cycle

1. Introduction

A disruptive way in which we engage with the fabrication of engineering parts and components is through the use of additive manufacturing (AM) technologies. AM can be described as a group of digital fabrication techniques that use three-dimensional virtual models built on computer-aided-design packages to inform 3D-printers that manufacture the objects of interest by directly depositing the parent material layer upon layer. This family of disruptive fabrication techniques allows engineers across a whole range of industries to make complex geometries in the form of components, connections and custom parts that would be challenging (if not impossible) for traditional subtractive techniques.

In this setting, thanks to the R&D work that has been done since the 1980s, nowadays it is possible to buy of the shelf 3D-printers that allow a variety of materials to be additively-manufactured effectively and at a relatively low cost, with the available 3D-printable materials including, amongst others, metals, polymers, composites and concrete.

As far as commercial 3D-printes are concerned, examination of the products available in the market suggests that the most widespread AM technologies are those suitable for additively manufacturing polymeric compounds. Amongst the different commercial polymers for AM, certainly polylactide (PLA) is the most commonly used. PLA can be used to fabricate a variety of objects such as, for instance, tool jigs, fixtures, and biomedical devices/implants [1]. PLA is a linear thermoplastic aliphatic biodegradable polyester that is made from natural primary sources such as, for instance, maize starch, manihot esculenta, or sugar cane.

In order to use components of additively manufactured (AM) PLA in situations of engineering interest, one of the key aspects is performing both static and fatigue assessment by always reaching an adequate level of accuracy and, therefore, of safety. In this context, the available technical literature makes it evident that in recent years the international scientific community has focussed its attention mainly on the mechanical behaviour and strength of AM PLA when this polymer is subjected to static loading (see Refs [3-10] and the references reported therein). In contrast, just a few studies dealing with the fatigue behaviour of 3D-printed PLA have been published so far [10-15].

As far as AM PLA's mechanical response under static loading is concerned, much experimental evidence suggests that its ultimate tensile strength (UTS) depends primarily on the following technological variables: layer thickness, infill level, filling pattern, filling rate, nozzle diameter, raster angle, feed rate, printing speed, and manufacturing temperature [2-8]. In this context, both the UTS and Young's modulus, E, of AM PLA are seen to increase as the raster angle decreases [3, 4], the σ_{UTS} vs. E relationship being just a simple linear function [4]. The stress vs. strain response of AM PLA is predominantly brittle. In other words, the mechanical behaviour of this 3D-printed polymer is characterised by a relatively low level of ductility, with the characteristics of the non-linear part of the total deformation varying as the raster angle changes [6, 7]. Further, the elastic behaviour displays a very low level of anisotropy, whereas the plastic response is not only ductile, but also orthotropic [5-7].

Compared to standard PLA, the AM process returns a polymer which has a relatively high value of the fracture toughness, a relatively low sensitivity to the rate of the applied loading,

and an asymmetrical behaviour in terms of mechanical response under tension/compression [5, 6]. Another important aspect is that the overall static strength of AM PLA is strongly influenced also by the pigments being used to colour the parent polymer [9].

This brief review of the state-of-the-art knowledge makes it evident that AM PLA's mechanical response/strength under static loading is rather complex. However, in terms of engineering static assessment, the problem can be simplified greatly by observing that the effect of both raster orientation and shell thickness on Young's modulus, UTS, and yield stress can be disregarded without much loss of accuracy [7, 8]. Accordingly, components made of AM PLA can be designed against static loading by simply treating this polymer as a homogenous and isotropic material [7, 10].

Turning to the fatigue behaviour of AM PLA, Letcher and Waytashek [11] performed an extensive experimental investigation involving a large number of samples that were fabricated (using 3D-printer "Makerbot Replicator 2x") by setting the raster angle equal to 0°, 45° and 90°. The fatigue tests were run under fully-reversed sinusoidal axial force with frequencies varying in the range 2-20 Hz. Similarly, Afrose et al. [12] used 3D printer "Cube-2" to additively manufacture a series of flat specimens, with the samples being made by setting the printing direction equal to 0°, 45° and 90°. These dog-bone flat specimens were tested under zero-tension cyclic axial loading at a frequency equal to 1 Hz.

Even if these two experimental investigations were based on specimens manufactured not only via different commercial 3D printers, but also by employing PLA coming from different suppliers, the two groups of researchers came to the final common conclusion that AM PLA's fatigue behaviour is somehow affected by the manufacturing direction. Along the same lines, by performing a more complex and articulated experimental investigation, Jerez-Mesa et al. [13] observed that, as per the static case, AM PLA's overall fatigue strength as well is influenced not only by the printing direction, but also by the nozzle size, the layer height, the in-fill level and the manufacturing rate. Owing to the complexities associated with the mutual interactions amongst these technological parameters, the main conclusion from this study was that the

only way to assess/quantify the influence of these key manufacturing variables on AM PLA's fatigue response is by running time-consuming and expensive *ad hoc* experiments [13].

In this complex scenario, this paper summarises the outcomes from a comprehensive experimental investigation that was run in the Structures Laboratory of the University of Sheffield to study systematically the influence on AM PLA's fatigue behaviour of raster orientation and non-zero mean stresses. In particular, the experiments being described in the following sections were run to define a unifying design curve suitable for performing the fatigue assessment of AM PLA components by simultaneously taking into account the influence of both 3D-printing direction and superimposed static stresses.

2. Materials and methods

The specimens tested in the Structures Laboratory of the University of Sheffield were additively manufactured through commercial 3D-printer Ultimaker 2 Extended+, with this printer making use of the fused deposition modelling technology. In more detail, a large number of dog-bone flat samples was fabricated by melting, through a nozzle, 2.85mm diameter-white wires of New Verbatim PLA that were unwound from coils. The polymer being extruded was deposited directly onto the build-plate to create layers of material, with the specific shape of each layer being obtained via the horizontal movement of the nozzle itself. By cooling and hardening after being deposited, the filaments of PLA stuck together in a single mass by attaching not only to each other, but also to the previous layer of material. After manufacturing a layer, the build-plate lowered creating the space needed to fabricate a new one. Any layer of PLA was manufactured by first building a perimetric wall (called "shell") that is used by the 3D-printer not only to contain the internal material, but also to reach a higher level of precision in terms of dimensions and shape. To avoid the formation of voids and defects during the manufacturing process, the thickness of the shell was set equal to the nozzle diameter (i.e., equal to 0.4 mm). All the fatigue specimens were manufactured flat on the build-plate, with the key variables of the 3D-printing process being as follows: nozzle temperature equal to 240°C, build-plate temperature to 60°C, print speed to 30 mm/s, infill

density to 100%, and layer height to 0.1 mm. These values for the key manufacturing parameters were chosen because are those recommended by the manufacturer of the 3D-printer being used to fabricate objects made of PLA.

The samples of AM PLA being tested were fabricated by setting manufacturing angle θ_p equal to 0°, 45°, and 90°. According to the schematic sketch of Fig. 1a, θ_p was defined as the angle between the longitudinal axis of the specimen being manufactured and the vertical axis of the built plate. Since 3D-printer Ultimaker 2 Extended+ fabricated the samples by depositing the filaments always at ±45° to the principal axis of the build-plate (Fig. 1a), the effect of the raster orientation on the fatigue strength of the AM polymer being tested was investigated by testing specimens manufactured by making angle θ_p vary in the range 0°-90°.

The dog-bone flat samples (Fig. 1b) manufactured according to the procedure briefly described above had net width equal to 6 mm and thickness equal to 3 mm and to 5 mm.

The fatigue results used in the present study were generated via an electric fatigue table that was modified and optimised for this specific experimental campaign (Fig. 1c), with this being done in order to adhere as much as possible to the pertinent recommendation of the ASTM [16, 17].

As per Fig. 1c, the sinusoidal axial load signal was gathered using a loading cell, whereas the resulting nominal displacement was monitored via a linear LVDT. Owing to the reduced dimensions of the specimens being tested, all the fatigue tests were run up to the complete breakage of the samples themselves. The experiments were run at room temperature by setting the load ratio, $R=\sigma_{min}/\sigma_{max}$, equal to -1, -0.5, 0, and 0.3 and the frequency to 10 Hz. Run out tests were stopped at $2 \cdot 10^6$ cycles. According to the recommendations of the Japan Society of Mechanical Engineers [18], the median S-N curves will be determined by testing 8 specimens for any investigated load ratio/geometry configuration. The S-N curves in the finite life region (i.e., in between $500 \div 2 \cdot 10^6$ cycles to failure) were attempted to be determined by testing at least two specimens at each of, at least, four different stress levels (i.e., testing with replicated data). The number of specimens being tested for any manufacturing/load ratio configuration being investigated are listed in Tab. 1.

3. Cracking behaviour and summary of the experimental results

In order to understand the role played by manufacturing angle θ_p and load ratio R, initially attention was focussed on the profiles and characteristics of the crack paths leading to the final breakage of the specimens being tested. As shown in Fig. 2, the cracking behaviour of the tested PLA was investigated by considering the crack initiation process as well as the subsequent crack growth phase.

According to the matrix of failures shown in Fig. 2, independently of printing direction θ_p and load ratio R, the crack initiation process was seen to take place always on material planes that were almost normal to the direction of the applied cyclic axial force. This suggests that the crack initiation phase was then driven by a Mode I-governed damage mechanism that resulted in initial cracks having length of the order of the shell thickness (i.e., having length equal to about 0.4 mm). This opening-mode dominated initiation process led then to the subsequent crack growth phase that occurred along zig-zag paths, where the profile of these paths followed the directions of the manufacturing filaments (Fig. 2). Thus, according to the pictures shown in Fig. 2, the hypothesis can be formed that, independently of printing direction θ_p and load ratio R, the crack growth process was governed by three concomitant failure mechanisms, i.e., (i) de-bonding between adjacent filaments, (ii) de-bonding between adjacent layers and (iii) rectilinear cracking of the filaments.

Turning to the fatigue strength data, all the results we generated are summarised in the SN diagrams of Fig. 3 for $\theta_p=0°$, of Fig. 4 for $\theta_p=30°$, and of Fig. 5 for $\theta_p=45°$. In these charts, for any experimental result, the amplitude of the applied stress, σ_a, is plotted against the resulting number of cycles to failure, N_f (on logarithmic scales). The associated scatter bands were calculated, for a probability of survival, P_S, equal to 90% and 10%, under the hypothesis of a log-normal distribution of the number of cycles to failure for each stress amplitude, with this being done by setting the confidence level invariably equal to 95% [19, 20]. It is important to point out here that this rigorous statistical procedure was used not only to build the SN diagrams reported in Figures 3 to 5, but also those shown/summarised in Figures 6 to 10.

Finally, for the sake of clarity, the fatigue curves being estimated for P_S=50% are also summarised in Table 1 (together with the corresponding values of σ_{UTS} [7]) in terms of negative inverse slope, k, endurance limit, $\sigma_{A, 50\%}$, extrapolated at N_{Ref}=2·10^6 cycles to failure and scatter ratio, T_σ, of the stress amplitude for 90% and 10% probabilities of survival.

4. Results and discussion

4.1. Influence of manufacturing direction

The results summarised in Figures 3 to 5 were initially used to investigate the influence of manufacturing direction θ_p on the overall fatigue strength of the AM polymer being tested. To this end, for a given value of the load ratio, R, the results generated by testing specimens manufactured with different values for angle θ_p were re-analysed together obtaining the scatter bands that are shown in Figure 6.

Strictly speaking, these SN diagrams confirm that, as observed by Letcher and Waytashek [11] as well as by Afrose et al. [12], manufacturing angle θ_p did affect the fatigue behaviour of the AM PLA being tested, although a univocal trend is not apparent. Nevertheless, the relatively low values for scatter ratio T_σ suggest that, as far as engineering fatigue assessment is concerned, the influence of manufacturing angle θ_p can be neglected, with this resulting just in a little loss of accuracy that would be in any case compensated by the usage of engineering safety factors. If this simplifying hypothesis is accepted for design purposes, then the hypothesis can be formed that fatigue assessment of components/parts made of AM PLA can be performed effectively by simply treating this polymer as a homogenous and isotropic material - i.e., without taking into account the effect of the raster angle.

To conclude, it is interesting to point out that this outcome was somehow expected since, under static loading as well, manufacturing angle is seen to have (from a design point of view) little effect on the overall strength of AM PLA [7, 8].

4.2. Effect of superimposed static stresses

Having investigated the influence of the raster angle, attention was then focused on the effect of non-zero mean stresses. This was done by taking as a starting point the trend that was observed by grouping together in the non-dimensional chart of Fig. 7 all the experimental results being generated. In more detail, this chart was built by plotting the ratio between the endurance limits under R≠-1 and the corresponding endurance limit generated under R=-1 against the ratio between mean stress σ_M (still in the endurance limit condition) and σ_{UTS}. In the same chart also those equations that are commonly used to assess the effect of non-zero mean stresses on the fatigue strength of metals [21, 22] are plotted for comparison purposes, where [21, 23]:

$$\sigma_A = \sigma_{A,R=-1} \left(\frac{\sigma_M}{\sigma_{UTS}} \right) \text{ - Goodman's relationship} \tag{1}$$

$$\sigma_A = \sigma_{A,R=-1} \left[1 - \left(\frac{\sigma_M}{\sigma_{UTS}} \right)^2 \right] \text{ - Gerber's parabola} \tag{2}$$

$$\sigma_A = \sigma_{A,R=-1} \sqrt{1 - \frac{\sigma_M}{\sigma_{UTS}}} \text{ - Dietman's parabola} \tag{3}$$

$$\sigma_A = \sigma_{A,R=-1} \sqrt{1 - \left(\frac{\sigma_M}{\sigma_{UTS}} \right)^2} \text{ - Elliptical relationship} \tag{4}$$

By directly comparing the experimental results generated under R>-1 to the classic formulas reported above it becomes apparent that, as far as AM PLA is concerned, the presence of non-zero mean stresses is associated with a more pronounced damaging effect than the one which is usually observed in metallic materials.

Taking as a starting point this outcome, an alternative solution to assess the detrimental effect of superimposed static stresses on the fatigue strength of AM PLA was attempted to be proposed by simply re-analysing the data reported in Figs 3 to 5 in terms of maximum value of the endurance limit extrapolated, for P_S=50%, at N_{Ref}=2·10^6 cycles to failure, $\sigma_{MAX, 50\%}$. In other words, the assumption was made that the mean stress effect in fatigue of AM PLA could

be modelled directly through the maximum stress in the cycle, where this could be done since, by definition, $\sigma_{max}=\sigma_m+\sigma_a$ already contains the mean stress information [24-26].

The $\sigma_{MAX,50\%}$ vs. $R=\sigma_{min}/\sigma_{max}$ diagram of Fig. 8a makes it evident that this simple and straightforward hypothesis resulted in a very low level of scattering, with the experimental results generated by investigating different values of θ_p and R all falling within two standard deviations, S_D, of the mean. In a similar way, the k vs. R graph reported in Fig. 8b confirms that also the negative inverse slopes associated with the different fatigue curves were all characterised by a very low level of scattering.

The fact that σ_{max} is a stress quantity suitable for modelling the mean stress effect in fatigue of AM PLA is further confirmed by SN diagram shown in Fig. 9. In this log-log chart all the experimental results being generated by making θ_p vary in the ranges $0°\div45°$ and R in the range $-1\div0.3$ were plotted together in terms of σ_{max}. Fig. 9 makes it evident that this simple approach based on the use of the maximum stress in the cycle allowed all the experimental data points to fall within a relatively narrow scatter band, i.e. a scatter band characterized by a T_σ ratio equal to about 2.9.

As per the re-analysis summarised in the present section (see Fig. 9), it is possible to conclude by observing that, from a fatigue design point of view, the effect of non-zero mean stresses on AM PLA can effectively be taken into account by simply performing the fatigue assessment in terms of maximum stress in the cycle, σ_{max}.

4.3. Unifying design curve

In order to propose a unifying design curve that can be used in situation of engineering interest to design AM PLA against fatigue, the results summarised in the SN charts of Figs 3 to 5 were plotted, in terms of σ_{max}, together with the experimental data generated by Letcher and Waytashek [11] as well as by Afrose et al. [12].

As to the data taken from the literature, it is useful to recall here that these two groups of researchers tested under cyclic loading flat dog-bone samples additively manufactured by

setting the raster angle equal to 0°, 45° and 90°. Letcher and Waytashek [11] tested their specimens (with 13 mm x 6 mm rectangular cross-section) under axial loading by setting the load ratio, R, invariably equal to -1 and by making the frequency vary in the range 2-20 Hz. The specimens manufactured by Afrose et al. [12] had instead net width equal to 10 mm and thickness equal to 4 mm and they were tested, in the low-cycle fatigue regime, under R=0 at a frequency of 1 Hz.

The experimental data produced by Letcher and Waytashek [11] as well as by Afrose et al. [12] were then plotted together with the new data summarised in Figs 3 to 5 to build the SN graph reported in Fig. 10. This log-log diagram plots the σ_{max} to σ_{UTS} ratio against the number of cycles to failure, N_f. As done for the previous statistical re-analyses, the scatter band shown in Fig. 10 (which is delimited by two straight lines that are characterised by a probability of survival, P_S, equal to 90% and 10%, respectively) was estimated under the hypothesis of a log-normal distribution of the number of cycles to failure for each stress level, with the confidence level being taken equal to 95% [19, 20].

According to the reasoning summarised in Sections 4 and 5, the SN chart of Fig. 10 confirms that, form an engineering fatigue design point of view, the fatigue behaviour of AM PLA is seen to be just marginally affected by the values of both the manufacturing angle and the load ratio, with the fatigue strength of this AM polymer being proportional to the ultimate tensile strength. This means that, similarly to what was observed under static loading [7, 8], the chart of Fig. 10 strongly supports the idea that, as long as the components of interest are manufactured flat on the build-plate, AM PLA can be designed again fatigue by simply treating this polymer as a homogenous and isotropic material.

To conclude, according to the statistical post-processing summarised in the log-log SN chart of Fig. 10, when appropriate experiments cannot be run, the following unifying design fatigue curve (valid for $P_S>90\%$) is recommended to be used to perform the fatigue assessment of AM PLA manufactured by setting the infill level equal to 100%:

$$k=5.5 \tag{5}$$

$\sigma_{MAX}=0.1 \cdot \sigma_{UTS}$ at $N_{Ref}=2 \cdot 10^6$ cycles to failure $\hspace{4cm}$ (6)

5. Conclusions

In the present paper a large number of new experimental results were re-analysed along with other data sets taken from the technical literature in order to investigate the effect of raster angle and non-zero mean stresses on the fatigue behaviour of AM PLA.

According to the outcomes from the research work summarised in the present paper, the most relevant conclusions are listed below, with these conclusions strictly applying to components of PLA that are additively manufactured flat on the build-plate.

- The cracking behaviour of AM PLA under fatigue loading is seen to be governed by the following three failure mechanisms: (i) rectilinear cracking of the filaments, (ii) de-bonding between adjacent filaments and (iii) de-bonding between adjacent layers.

- As per the static case, under fatigue loafing as well the effect of the orientation of the filaments on the fatigue behaviour of AM PLA can be neglected with little loss of accuracy. Therefore, from a fatigue design point of view, AM PLA can be treated as a homogenous and isotropic material.

- The detrimental effect of superimposed static stresses on AM PLA's fatigue strength can be quantified and assessed by addressing the design problem in terms of maximum stress in the cycle.

- If a specific fatigue curve for the AM PLA polymer being used is not available, then fatigue assessment can be performed (for $P_S \geq 90\%$) via a unifying design curve having negative inverse slope equal to 5.5 and endurance limit at $2 \cdot 10^6$ cycles to failure equal to $0.1 \cdot \sigma_{UTS}$.

- Systematic experimental work should be done in order to investigate the effect of the in-fill level on the fatigue strength of 3D-printed PLA;

- More work needs to be done in this area to investigate the effect of the key AM manufacturing variables on the fatigue strength of notched components of AM PLA.

References

[1] Ngo TD, Kashani A, Imbalzano G, Nguyen KTQ, Hui D. Additive manufacturing (3D printing): A review of materials, methods, applications and challenges. Compos Part B-Eng 2018;143(15):172-196.

[2] Ciurana JD. Selecting process parameters in RepRap additive manufacturing system for PLA scaffolds manufacture. Procedia CIRP 2013;5:152-157.

[3] Lanzotti A, Grasso M, Staiano G, Martorelli M. The impact of process parameters on mechanical properties of parts fabricated in PLA with an open-source 3-D printer. Rapid Prototyping J 2015;21(5):604-617.

[4] Casavola C, Cazzato A, Moramarco V, Pappalettere C. Orthotropic mechanical properties of fused deposition modelling parts described by classical laminate theory. Mater Des 2016;90;453-458.

[5] Chacón JM, Caminero MA, García-Plaza E, Núñez PJ. Additive manufacturing of PLA structures using fused deposition modelling: Effect of process parameters on mechanical properties and their optimal selection. Mater Des 2017;124:143-157.

[6] Song Y, Li Y, Song W, Yee K, Lee K-Y, Tagarielli VL. Measurements of the mechanical response of unidirectional 3D-printed PLA. Mater Des 2017;123:2017:154-164.

[7] Ahmed AA, Susmel L. A material length scale based methodology to assess static strength of notched additively manufactured polylactide (PLA). Fatigue Fract Eng Mater Struct 2018;41(10):2071-2098.

[8] Ahmed AA, Susmel L. Static assessment of plain/notched polylactide (PLA) 3D-printed with different in-fill levels: equivalent homogenised material concept and Theory of Critical Distances. Fatigue Fract Eng Mater Struct. 2019;(42):883–904.

[9] Wittbrodt B, Pearce JM. The effects of PLA color on material properties of 3-D printed components. Additive Manufacturing 2015;8:110-116.

[10] Ezeh OH, Susmel L. Reference strength values to design against static and fatigue loading polylactide additively manufactured with in-fill level equal to 100%. Mat Design Process Comm. 2019;e45. https://doi.org/10.1002/mdp2.45.

[11] Letcher T, Waytashek M. Material property testing of 3D-printed specimen in PLA on an entry-level 3D-printer. In: Proceedings of the ASME 2014 International Mechanical Engineering Congress & Exposition (IMECE2014), 14-20 November 2014, Montreal, Quebec, Canada, IMECE2014-39379.

[12] Afrose F, Masood SH, Iovenitti P, Nikzad M, Sbarski I. Effects of part build orientations on fatigue behaviour of FDM-processed PLA material. Prog Addit Manuf 2016;1:21-28.

[13] Jerez-Mesa R, Travieso-Rodriguez JA, Llumà-Fuentes J, Gomez-Gras G, Puig D. Fatigue lifespan study of PLA parts obtained by additive manufacturing. Procedia Manufacturing 2017;13:872-879.

[14] Ezeh OH, Susmel L. On the fatigue strength of 3D-printed polylactide (PLA). Procedia Structural Integrity 2018;29-36:2018.

[15] Ezeh, OH, Susmel L. Fatigue behaviour of additively manufactured polylactide (PLA). Procedia Structural Integrity 2018;13:728-734.

[16] Anon. Standard Test Method for Uniaxial Fatigue Properties of Plastics. ASTM D7791; 2017.

[17] Anon. Standard Practice for Conducting Force Controlled Constant Amplitude Axial Fatigue Tests of Metallic Materials. ASTM E466; 2011.

[18] Anon. Japan Society of Mechanical Engineers, Standard method of statistical fatigue testing. JSME S 002-1981, 1981

[19] Al Zamzami I, Susmel L. On the accuracy of nominal, structural, and local stress based approaches in designing aluminium welded joints against fatigue. Int J Fatigue 2017;101:137-158.

[20] Spindel JE, Haibach E. Some considerations in the statistical determination of the shape of S-N cruves. In: Statistical Analysis of Fatigue Data, ASTM STP 744 (Edited by Little, R. E. and Ekvall, J. C.), pp. 89–113, 1981.

[21] Iurzolla E. I criteri di resistenza. Ed. Libreria Cortina, Padova, Italy 1991 (in Italian).

[22] Susmel L. Multiaxial notch fatigue: from nominal to local stress–strain quantities. Cambridge (UK): Woodhead & CRC; 2009.

[23] Susmel L, Tovo R, Lazzarin P. The mean stress effect on the high-cycle fatigue strength from a multiaxial fatigue point of view. Int J Fatigue 2005;27:928-943.

[24] Socie DF. Multiaxial Fatigue Damage Models. Trans ASME - J Eng Mat Techn 1987;109:293-298.

[25] Susmel L. A unifying methodology to design un-notched plain and short-fibre/particle reinforced concretes against fatigue. Int J Fatigue 2014;61:226–243.

[26] Jadallah O, Bagni C, Askes H, Susmel L. Microstructural length scale parameters to model the high-cycle fatigue behaviour of notched plain concrete. Int J Fatigue 2016;82:708-720.

Tables

θ_p [°]	σ_{UTS} [MPa]	N. of tests	R	k	$\sigma_{A,50\%}$ [MPa]	T_σ
0	42.6	15	-1	7.7	10.4	1.185
		15	-0.5	8.9	10.1	1.266
		12	0	7.4	6.1	1.592
		14	0.3	7.0	5.1	1.216
30	40.9	16	-1	4.3	4.5	1.911
		11	-0.5	7.2	5.5	1.498
		9	0	6.9	4.7	1.699
		9	0.3	5.8	3.3	2.174
45	42.5	11	-1	6.5	6.3	1.355
		10	-0.5	7.6	6.0	1.399
		11	0	7.5	4.7	1.302
		10	0.3	6.7	3.1	1.882

Table 1. Summary of the experimental results.
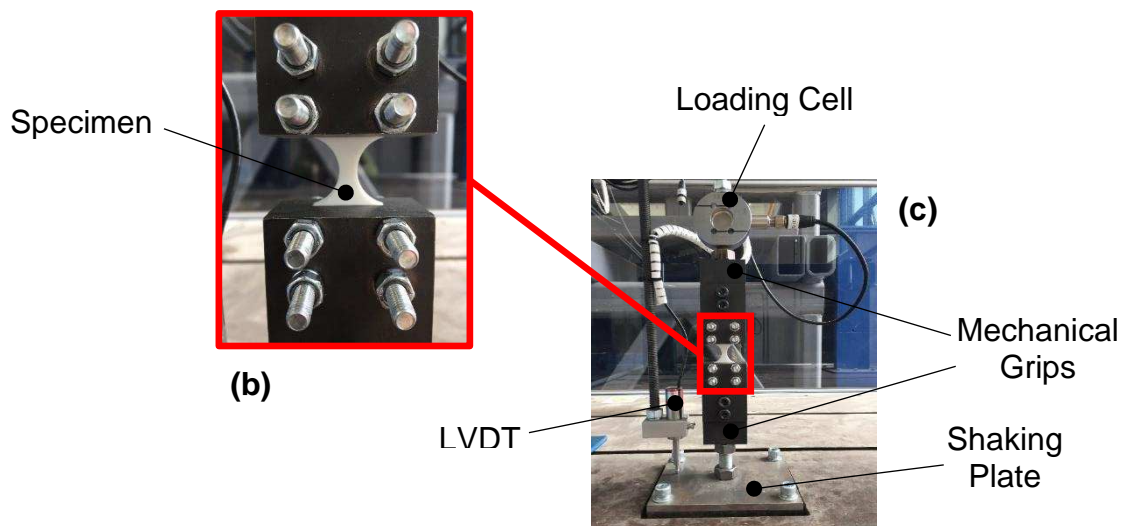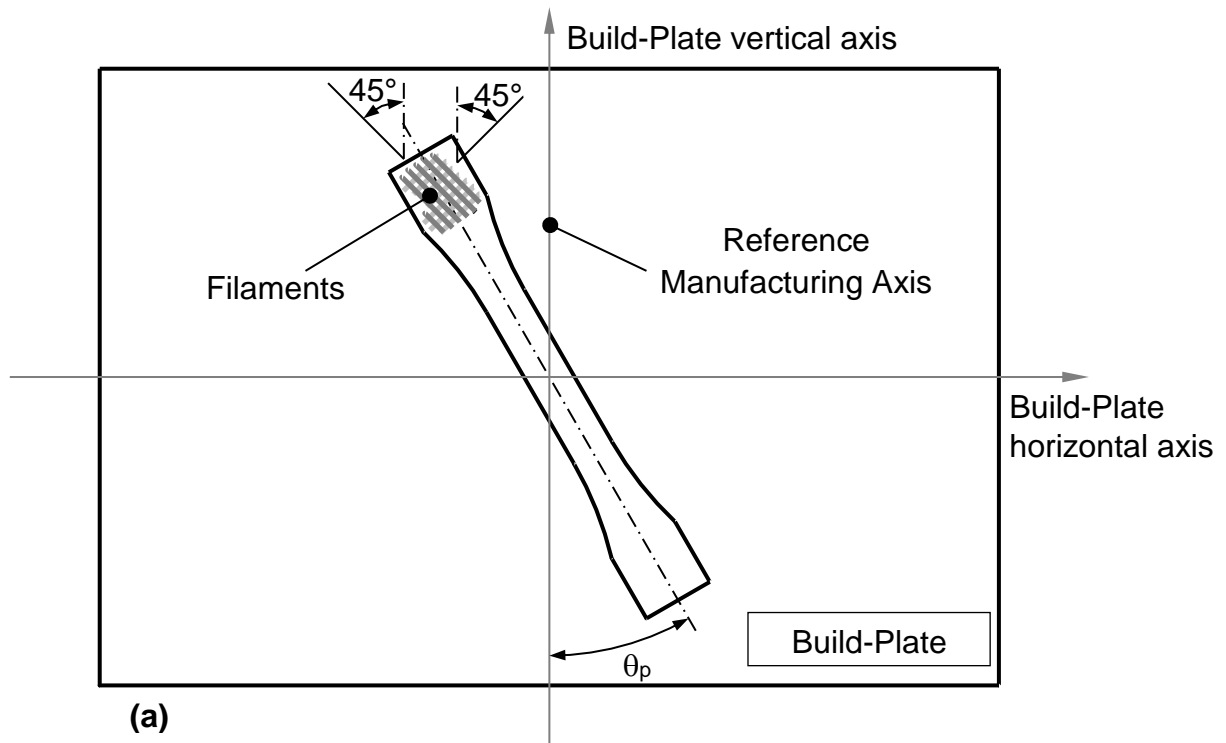
Figure 1. Definition of manufacturing angle θ_p (a); dog-bone fatigue specimens and clamping grips (b); overview of the electric fatigue table (c).
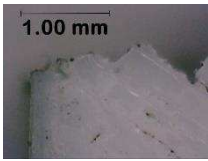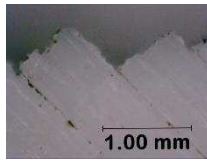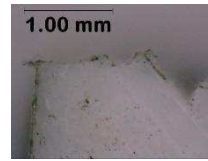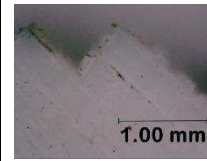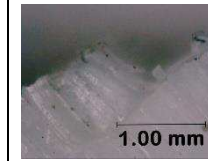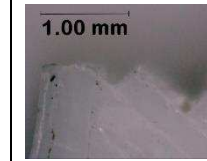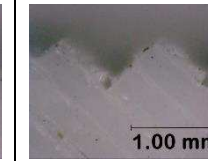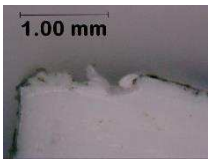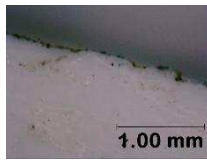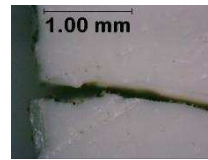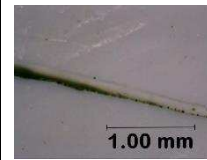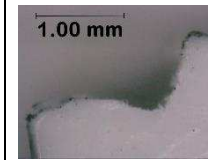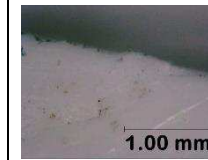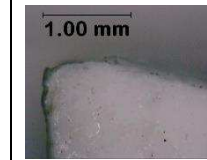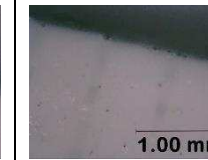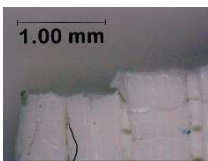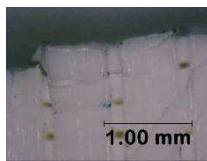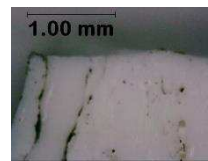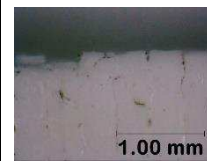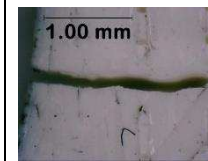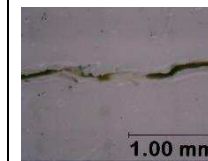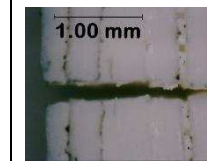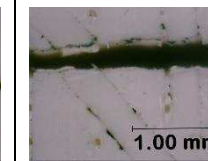
θ_p [°]	R=-1		R=-0.5		R=0		R=0.3	
	Initiation	Propagation	Initiation	Propagation	Initiation	Propagation	Initiation	Propagation
0								
	σ_a=20.2 MPa; N_f=10935 cycles		σ_a=20.6 MPa; N_f=2200 cycles		σ_a=14.0 MPa; N_f=4160 cycles		σ_a=9.4 MPa; N_f=24295 cycles	
30								
	σ_a=9.6 MPa; N_f=95090 cycles		σ_a=18.2 MPa; N_f=400 cycles		σ_a=5.7 MPa; N_f=427325 cycles		σ_a=10.3 MPa; N_f=4120 cycles	
45								
	σ_a=15.3 MPa; N_f=8250 cycles		σ_a=7.3 MPa; N_f=1089866 cycles		σ_a=7.0 MPa; N_f=96795 cycles		σ_a=5.8 MPa; N_f=83890 cycles	

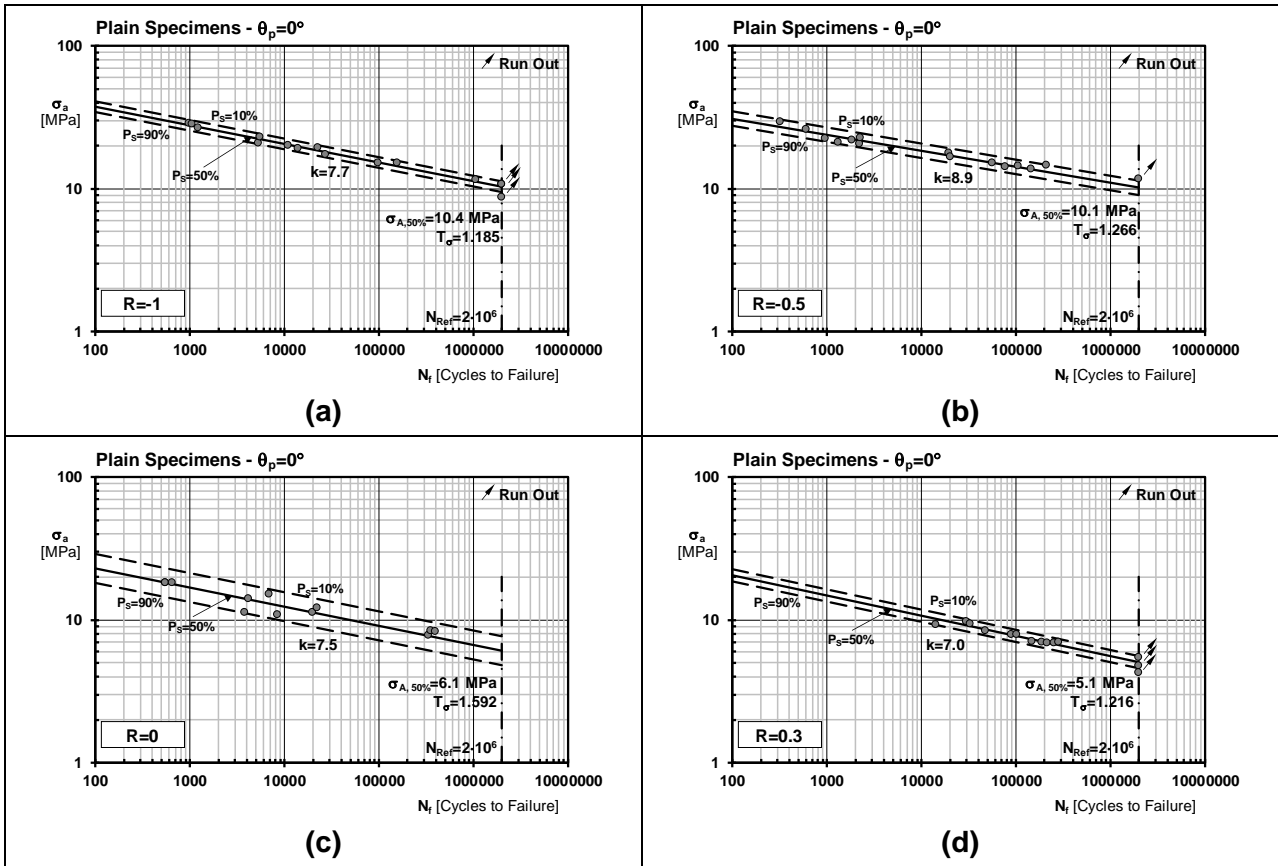**Figure 2.** Observed cracking behaviour (in the pictures the longitudinal axis of the specimens is oriented vertically).

Figure 3. SN diagrams summarising the results generated by testing specimens additively manufactured by setting manufacturing angle, θ_P, equal to $0°$.
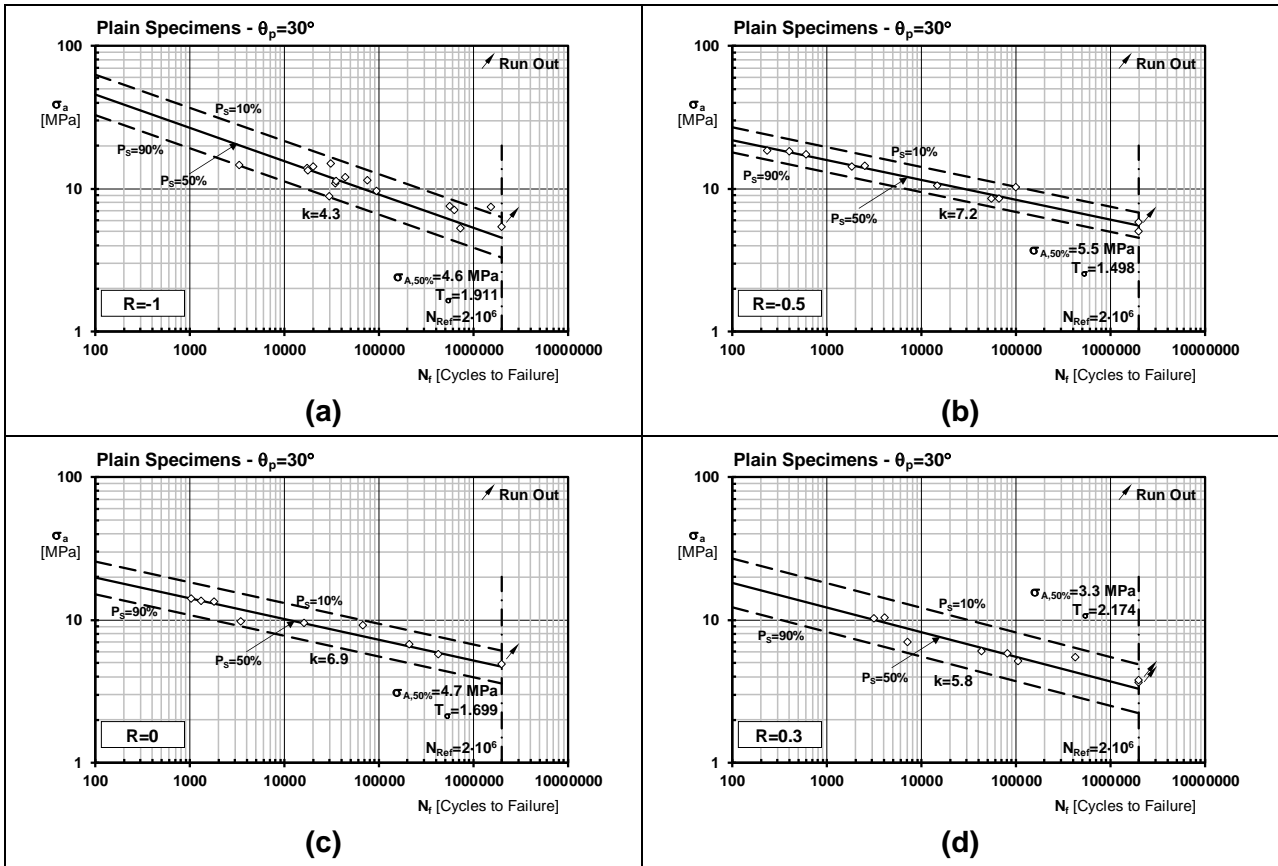
Figure 4. SN diagrams summarising the results generated by testing specimens additively manufactured by setting manufacturing angle, θ_P, equal to 30°.
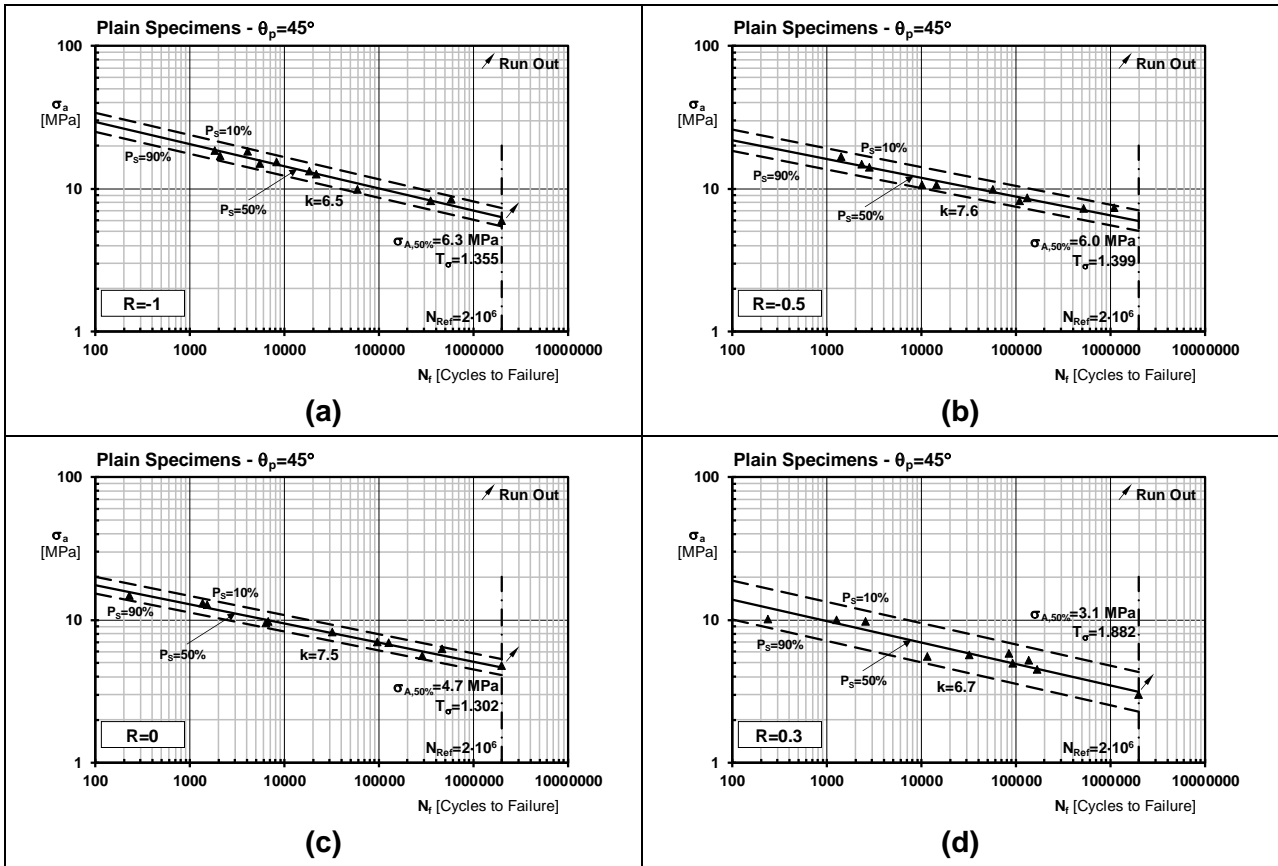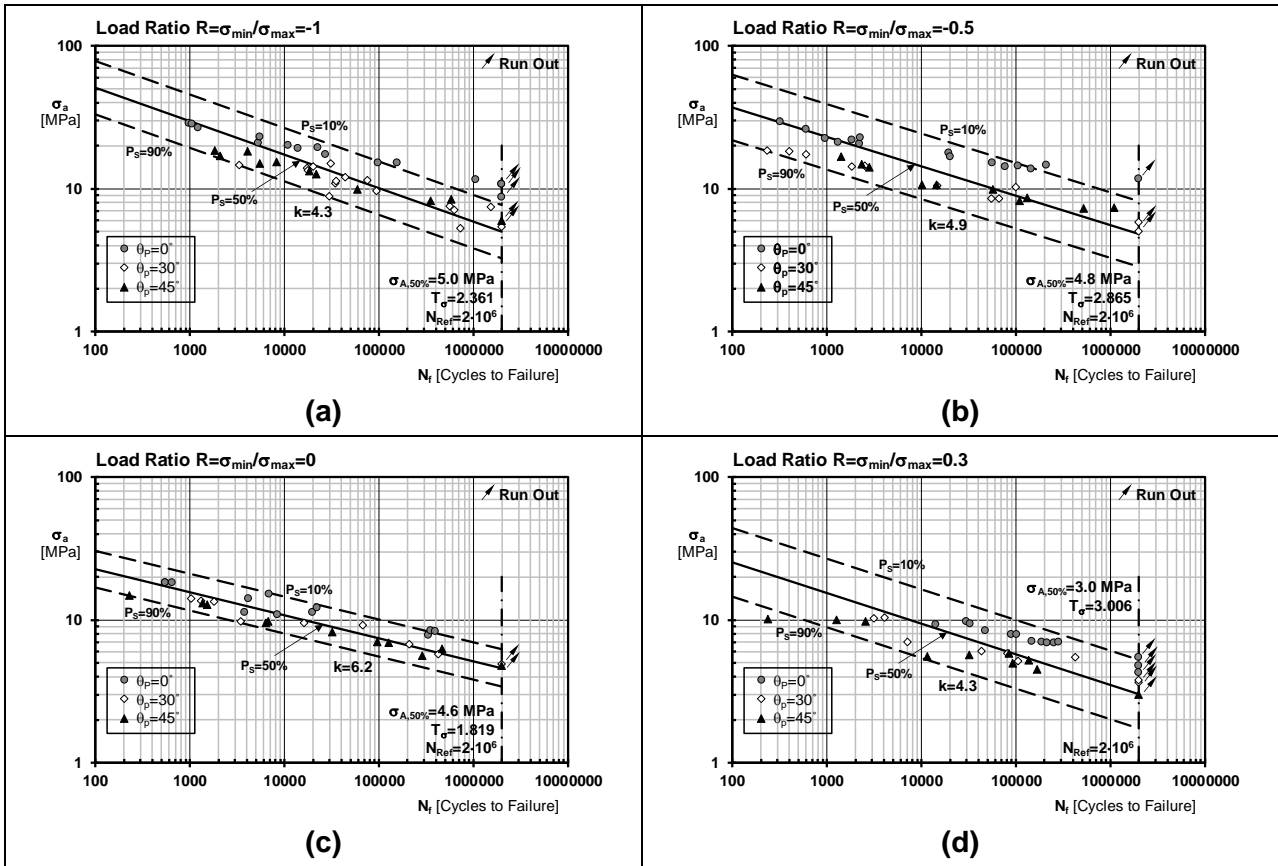
Figure 5. SN diagrams summarising the results generated by testing specimens additively manufactured by setting manufacturing angle, θ_P, equal to 45˚.

Figure 6. SN diagrams built by disregarding, for any investigated value of the load ratio, the influence of manufacturing angle θ_P.
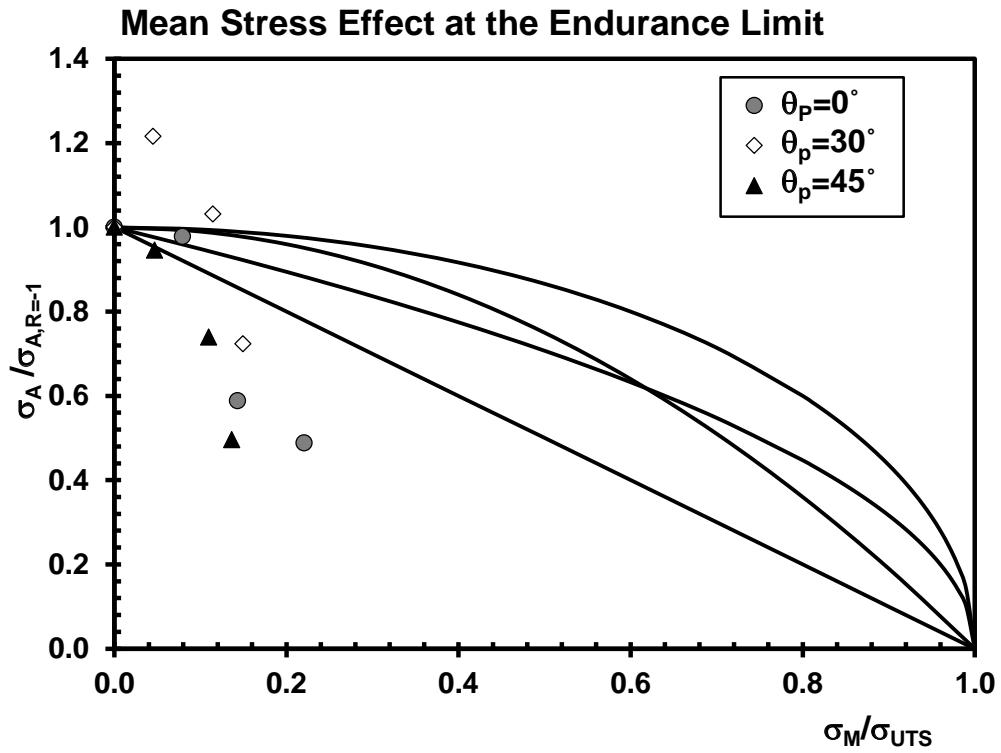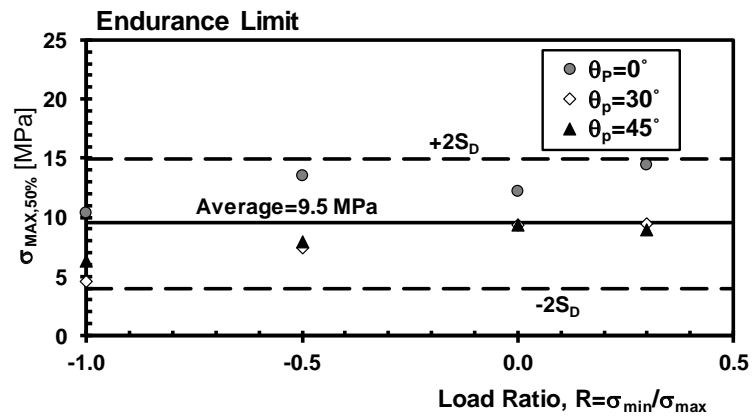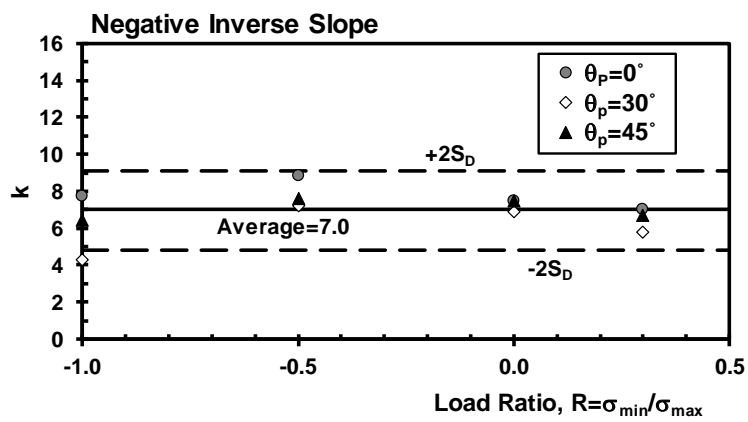
Figure 7. Accuracy of some standard relationships in assessing the effect of non-zero mean stresses on the fatigue strength of the PLA specimens being tested.

Figure 8. Effect of the load ratio, R, on the endurance limit (at $N_{Ref}=2 \cdot 10^6$ cycles to failure) expressed in terms of maximum stress in the cycles (a) as well as on the negative inverse slope, k, of the fatigue curves being generated (b).
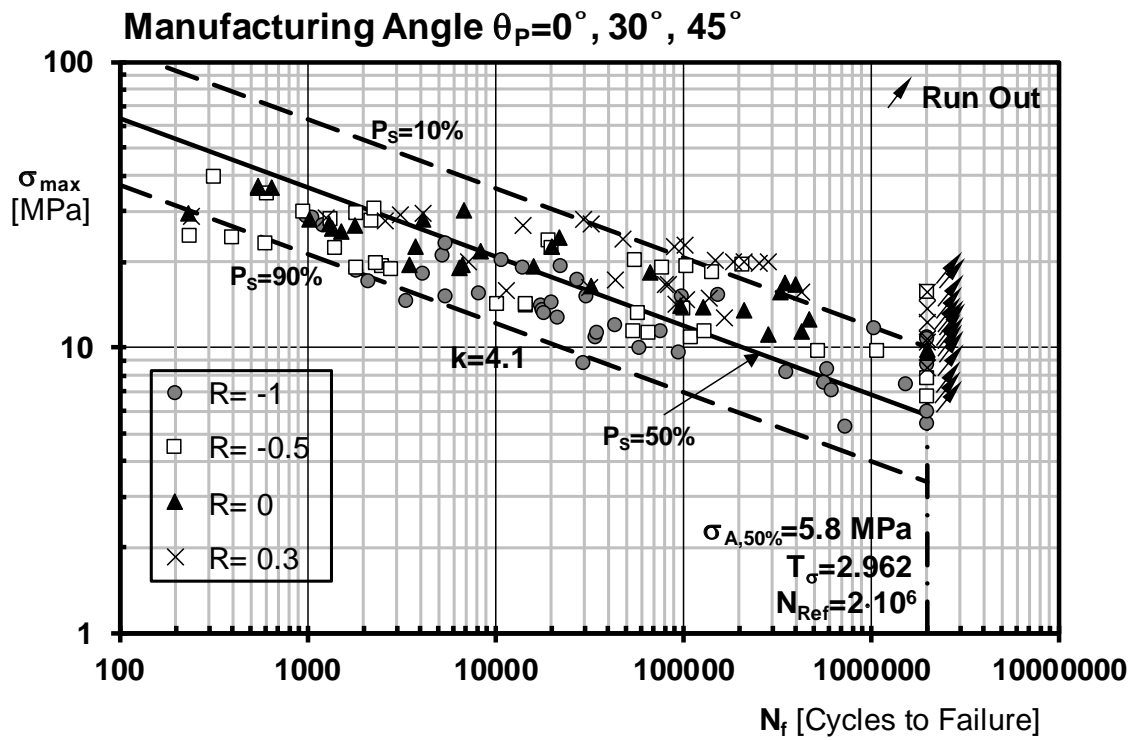
Figure 9. σ_{max} vs. N_f SN diagram summarising the fatigue data generated by testing, under load ratios equal to -1, -0.5, 0, and 0.3, plain specimens of PLA 3D-printed by setting the manufacturing angle, θ_P, equal to 0°, 30°, and 45°.
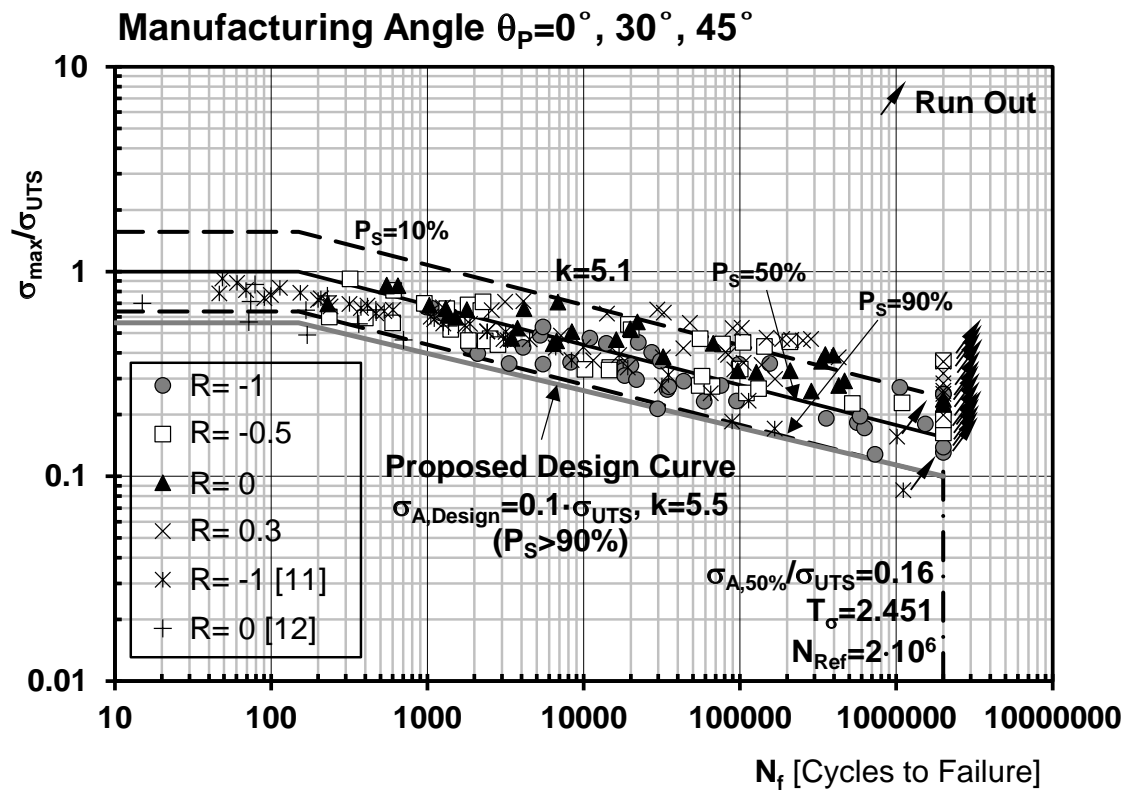
Figure 10. Unifying SN curve recommended to design additively manufactured PLA against fatigue.